

**Dieses Dokument ist eine Zweitveröffentlichung (Verlagsversion) /
This is a self-archiving document (published version):**

Stefan Schmult, Victor V. Solovyev, Steffen Wirth, Andreas Großer, Thomas Mikolajick,
Igor V. Kukushkin

**Magneto-optical confirmation of Landau level splitting in a GaN/AlGaN
2DEG grown on bulk GaN**

Erstveröffentlichung in / First published in:

Journal of vacuum science & technology / B. 2019, 37(2), Art.-Nr. 021210 [Zugriff am:
06.09.2022]. AIP Publishing. ISSN 2166-2746.

DOI: <https://doi.org/10.1116/1.5088927>

Diese Version ist verfügbar / This version is available on:

<https://nbn-resolving.org/urn:nbn:de:bsz:14-qucosa2-811000>

Magneto-optical confirmation of Landau level splitting in a GaN/AlGaN 2DEG grown on bulk GaN

Cite as: J. Vac. Sci. Technol. B **37**, 021210 (2019); <https://doi.org/10.1116/1.5088927>

Submitted: 15 January 2019 . Accepted: 26 February 2019 . Published Online: 11 March 2019

Stefan Schmult, Victor V. Solovyev, Steffen Wirth, Andreas Großer,  Thomas Mikolajick, and Igor V. Kukushkin

COLLECTIONS

Paper published as part of the special topic on [Conference Collection: 34th North American Molecular Beam Epitaxy Conference 2018](#)



View Online



Export Citation



CrossMark

ARTICLES YOU MAY BE INTERESTED IN

[Electron spin resonance in a 2D system at a GaN/AlGaN heterojunction](#)

Applied Physics Letters **113**, 052102 (2018); <https://doi.org/10.1063/1.5041363>

[Control of unintentional oxygen incorporation in GaN](#)

Journal of Vacuum Science & Technology B **35**, 02B104 (2017); <https://doi.org/10.1116/1.4975925>

[Critical parameters for the presence of a 2DEG in GaN/Al_xGa_{1-x}N heterostructures](#)

AIP Advances **9**, 125018 (2019); <https://doi.org/10.1063/1.5126917>



Advance your science and
career as a member of

AVS

LEARN MORE



Magneto-optical confirmation of Landau level splitting in a GaN/AlGaN 2DEG grown on bulk GaN

Stefan Schmult,^{1,a)} Victor V. Solovyev,² Steffen Wirth,³ Andreas Großer,⁴ Thomas Mikolajick,^{1,4} and Igor V. Kukushkin^{2,5}

¹TU Dresden, Electrical and Computer Engineering, Institute of Semiconductors and Microsystems, Nöthnitzer Str. 64, 01187 Dresden, Germany

²Institute of Solid State Physics RAS, 142432 Chernogolovka, Moscow District, Russia

³Max-Planck-Institute for Chemical Physics of Solids, Nöthnitzer Str. 40, 01187 Dresden, Germany

⁴NamLab gGmbH, Nöthnitzer Str. 64, 01187 Dresden, Germany

⁵National Research University Higher School of Economics, 101000 Moscow, Russia

(Received 15 January 2019; accepted 26 February 2019; published 11 March 2019)

Landau level splitting in a two-dimensional electron gas (2DEG) confined in an ultrapure GaN/AlGaN heterostructure grown by molecular beam epitaxy on bulk GaN is verified spectroscopically. The Landau level fan reconstructed from magneto-photoluminescence (PL) data yields an effective mass of $0.24m_0$ for the 2D electrons. Narrow excitonic PL line widths $< 100 \mu\text{eV}$, an atomically flat surface of the layer stack, as well as the absence of the 2DEG in the dark environment, are important ancillary experimental findings while focusing on magneto-PL investigations of the heterostructure. Simultaneously recorded Shubnikov-de Haas and magneto-PL intensity oscillations under steady UV illumination exhibit an identical frequency and allow for two independent ways of determining the 2D density. Published by the AVS. <https://doi.org/10.1116/1.5088927>

I. INTRODUCTION

While gallium nitride (GaN) based devices mature and increasingly emerge in power and high-frequency applications,^{1,2} inherent material properties such as a large bandgap of 3.4 eV, a large electron g-factor of ~ 2 (Ref. 3), and a large effective mass of $\sim 0.2m_0$, combined with high electron mobilities in two-dimensional electron gases (2DEGs) in excess of $10^5 \text{ cm}^2/\text{Vs}$ (Ref. 4), allow access to a new regime of meso- and macroscopic physics compared with gallium arsenide (GaAs).^{5,6} Landau level (LL) splitting of the density of states at moderate magnetic fields ($\sim 1 \text{ T}$), for example, is a hallmark of high-quality 2DEGs confined in semiconductor heterostructures. In magnetotransport experiments, LL splitting gives rise to Shubnikov-de Haas (SdH) oscillations in the longitudinal resistance. Minima in the longitudinal resistance occur at magnetic field values, at which the magnetic field-dependent density of states at the Fermi level exhibits a minimum. For large enough magnetic fields, the density of states can even become zero, which in turn results in zero longitudinal resistance and the well-known quantized and universal values of the Hall voltage.⁷ The optical detection of LLs in photoluminescence (PL) experiments manifests itself as a direct mapping of the Fermi distribution function, originating from the recombination of electrons from all occupied conduction band states to nondispersive hole states in the valence band. LL splitting in magneto-PL experiments was verified for 2DEGs confined in GaAs-based⁸ and zinc oxide (ZnO)-based⁹ heterostructures. Experimental observation of 2DEG-related PL features was

mentioned previously for GaN/AlGaN heterostructures;^{10–13} however, some of the reported energy positions caused noticeable controversy.¹⁴

Here, LL splitting in the density of states of 2D electrons confined at an ultrapure GaN/AlGaN interface is reported. From the resulting LL fan, an effective electron mass of $0.24m_0$ is extracted. In addition, using a Hall bar device allowed for simultaneous measurements of SdH oscillations in magnetotransport and oscillations of the magneto-PL intensity. These two independent measurements result in identical $1/B$ oscillation frequencies and thus give rise to identical electron densities.

II. EXPERIMENT

Detailed explanations on the sample growth and processing as well as on the measurement procedures and setups used will be given in Secs. II A and II B.

A. MBE growth and lateral Hall bar device processing

The discussed GaN/AlGaN heterostructure was grown in a customized VG V80H molecular beam epitaxy (MBE) system reaching a base pressure $< 10^{-10}$ mbar. The layer stack (presented in Fig. 1) consists of $1 \mu\text{m}$ GaN and 16 nm $\text{Al}_{0.06}\text{Ga}_{0.94}\text{N}$ barrier material capped with 3 nm GaN. It was grown at a rate of 240 nm/h on a 650 nm thick, dislocation-lean ($< 10^5 \text{ cm}^{-2}$) and a 2-in., hexagonal, Ga-polar GaN bulk substrate at a growth temperature of $\sim 700 \text{ }^\circ\text{C}$. This is slightly below the rapid Ga desorption point. The resulting 2DEG is located at the GaN/AlGaN interface. The source materials Ga and Al with purities of 8N and 6N5, respectively, were evaporated from single-filament effusion sources. Active nitrogen was supplied from an inductively coupled radiofrequency plasma source fed with purified nitrogen at a nominal

Note: This paper is part of the Special Topic Collection from 34th North American Molecular Beam Epitaxy Conference 2018.

^{a)}Electronic mail: stefan.schmult@tu-dresden.de

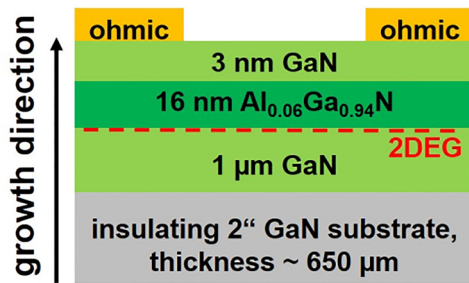


Fig. 1. Schematic of the investigated GaN/AlGaIn stack (not to scale). The MBE growth sequence starts with a $1\ \mu\text{m}$ thick GaN layer, followed by a $16\ \text{nm}$ thick AlGaIn barrier and a $3\ \text{nm}$ thick GaN cap layer. A 2DEG can be generated at the GaN/AlGaIn interface in the MBE material with the electron wave function predominantly localized in the GaN layer.

purity of 10N. The sample was rotated during growth at 10 rpm. Following a trend previously described in detail,^{15,16} the only traceable unintentional impurity in the GaN material grown by this procedure is oxygen. Its level was determined to $2 \cdot 10^{16}\ \text{cm}^{-3}$ by secondary ion mass spectroscopy in reference samples. Routinely, samples grown in our laboratory are screened with respect to their structural properties by atomic force microscopy (AFM, DI/Veeco DIMENSION 3100 operated in contact mode) and high-resolution x-ray diffraction (Bruker D8 Discover) before and after growth. Immediate consequences of the growth of ultrapure GaN/AlGaIn material on dislocation-lean GaN substrates on structural, optical, and electrical sample properties will be discussed in Sec. III A.

On small pieces of the 2-in. wafer, Hall bars were lithographically defined and mesa structures were patterned in a reactive ion etch step using a chlorine-based plasma. Ti/Al/Ni/Au stacks annealed at $800\ ^\circ\text{C}$ in the nitrogen atmosphere (6N) for 30 s serve as ohmic contacts. Typical dimensions of the Hall bars are $1.5\ \text{mm}$ and $500\ \mu\text{m}$ in length and width, respectively, to facilitate the PL signal acquisition.

B. Magnetotransport and magneto-PL setups

A Physical Property Measurement System by Quantum Design Inc. with a home-made optical access was used to perform temperature- and illumination-dependent magneto-transport measurements between 2 and 300 K. A standard low-frequency (17 Hz) lock-in technique with an excitation current of 100 nA was employed.

Magnetotransport and magneto-PL studies below 1 K were executed in ^3He cryostat equipped with a superconducting magnet reaching 15 T. The entire Hall bar was uniformly photoexcited with a HeCd laser at 325 nm wavelength via a bare fiber end. The distance of $\sim 20\ \text{mm}$ between the bare fiber end (numeric aperture = 0.22) and the sample surface ensures good homogeneity of both the illumination and the resulting 2DEG density as confirmed by the onset of SdH oscillations. The photoexcitation power was attenuated by optical filters and measured at the fiber input, and the fiber optical transmission amounts to $\sim 80\%$. Magnetotransport traces were recorded using a low-frequency lock-in technique.

To acquire PL data, light from the sample was collected with a second fiber in close proximity to the sample and then sent through a $1\ \text{m}$ focal length monochromator with an 1800 lines/mm grating. The second diffraction order of the dispersed light was detected by a deeply cooled CCD detector. The overall spectral resolution of the setup amounts to $70\ \mu\text{eV}$ as verified with atomic neon transition lines. The penetration depth of the exciting ultraviolet (UV) radiation allows for probing the 2DEG at the GaN/AlGaIn interface as well as sections of the $1\ \mu\text{m}$ thick MBE GaN layer. The excitation does not reach the GaN substrate, which is located at a depth of $1\ \mu\text{m}$ below the surface.

III. EXPERIMENTAL FINDINGS AND DISCUSSION

A. Consequences of the growth of ultrapure GaN/AlGaIn material on dislocation-lean GaN

Before focusing on the magnetic field-dependent photoluminescence and transport properties of the investigated heterostructure, some results immediately arising from the growth of the ultrapure GaN/AlGaIn stack on defect-lean material should be addressed.

As a result of the low areal defect density, AFM scans over macroscopic distances ($5\ \mu\text{m} \times 5\ \mu\text{m}$) do not show any surface defect decoration such as pits or hillocks, which are typical for screw and mixed-type dislocations.¹⁷ Alongside such smooth surfaces, monolayer steps of $\sim 0.25\ \text{nm}$ in height originating from slight crystallographic misorientations of the substrate surface become visible.

The next finding, attributed to the bulk character of the GaN substrate, is the excited states and narrow PL line widths of the donor-bound exciton transition at $\sim 10\ \text{meV}$ below the free exciton (A) transition in PL spectra at zero magnetic field (Fig. 2). Experimentally, a full width at half maximum of $\sim 100\ \mu\text{eV}$ for the most intense line around $3.47\ \text{eV}$ was confirmed (inset of Fig. 2). Due to the setup

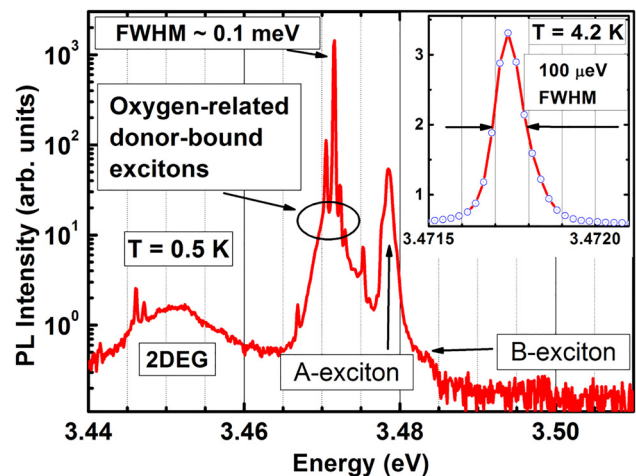


Fig. 2. Low-temperature PL data around the excitonic transition of the ultrapure GaN/AlGaIn heterostructure. The free exciton transitions at $3.48\ \text{eV}$ and the donor-bound transitions around $3.47\ \text{eV}$ originate from the $1\ \mu\text{m}$ thick GaN MBE layer. The inset shows high-resolution data of the most intense line around $3.4717\ \text{eV}$, exhibiting a line width of $\sim 100\ \mu\text{eV}$. The PL band around $3.45\ \text{eV}$ can be attributed to the 2DEG confined at the GaN/AlGaIn interface.

resolution of $70\mu\text{eV}$, the true line width of this transition is likely even narrower and among one of the smallest values ever reported for GaN.¹⁸ Yellow luminescence around 2.2 eV (not shown) is practically absent, consistent with its intensity dependence on the incorporated oxygen concentration as recently suggested.¹⁹ Around 3.45 eV, a rather broad spectral feature is visible, which is attributed to the 2DEG and explained in detail in Sec. III B.

Finally, the 2DEG is not present in the dark at temperatures between 0.5 and 300 K, as investigated in detail recently.²⁰ This behavior is attributed to the low unintentional donor level (oxygen at $2 \cdot 10^{16}\text{cm}^{-3}$). However, a 2DEG can be generated optically by UV illumination or electrostatically. At low temperatures, the 2DEG persists after UV excitation and subsequent blanking of the radiation. Under steady illumination at low temperatures, the 2D electron density depends only weakly on the excitation power.

B. Landau level splitting in the 2DEG verified by magneto-PL

The broad spectral feature at 3.45 eV in Fig. 2 is absent when recording PL from GaN layers without the AlGaN barrier layer. In case this feature represents the Fermi distribution at $B=0$, a width of $\sim 20\text{meV}$ corresponds to a 2DEG density of $\sim 2 \cdot 10^{12}\text{cm}^{-2}$, which is expected for the discussed layer stack containing a low Al mole fraction of only 6% in the barrier.²¹ By applying a magnetic field perpendicular to the 2DEG, peaks arising between 3.45 and 3.46 eV above 10 T clearly split proportional to the magnetic field (Fig. 3, upper panel), as expected for LLs. These peaks are unambiguously attributed to split Landau levels of the 2DEG, which is better seen in a contour plot of the PL intensity versus magnetic field and energy (Fig. 3, lower panel). At a fixed magnetic field above 10 T, multiple bright spots are visible. If the intensity maxima positions are plotted versus the magnetic field, an almost text-book-like Landau level fan can be reconstructed (Fig. 4). From the energy splitting associated with the Landau levels, an effective mass of $0.24m_0$ is extracted. The magnetic field-dependent intensity oscillations following the dashed line in Fig. 3, lower panel, will be discussed in more detail in Sec. III C.

C. Simultaneously detected oscillations in magneto-PL intensity and longitudinal magnetoresistance

While the focus in Sec. III B was on the PL intensity maxima at fixed magnetic field representing LL splitting, we now turn to the magnetic field-dependent PL intensity variations along a selected LL, in particular the lowest one. The lowest LL is indicated by the dashed line in Fig. 3, lower panel. The PL intensity shows oscillatory behavior similar to the well-known SdH oscillations (Fig. 5, upper panel). The magneto-PL oscillations were simultaneously recorded with its magnetotransport counterpart from the same Hall bar device at $T=0.5\text{K}$ under steady UV illumination at $70\mu\text{W}$. The onset of the SdH oscillations in the longitudinal resistance is observed at $<2\text{T}$, representing decent

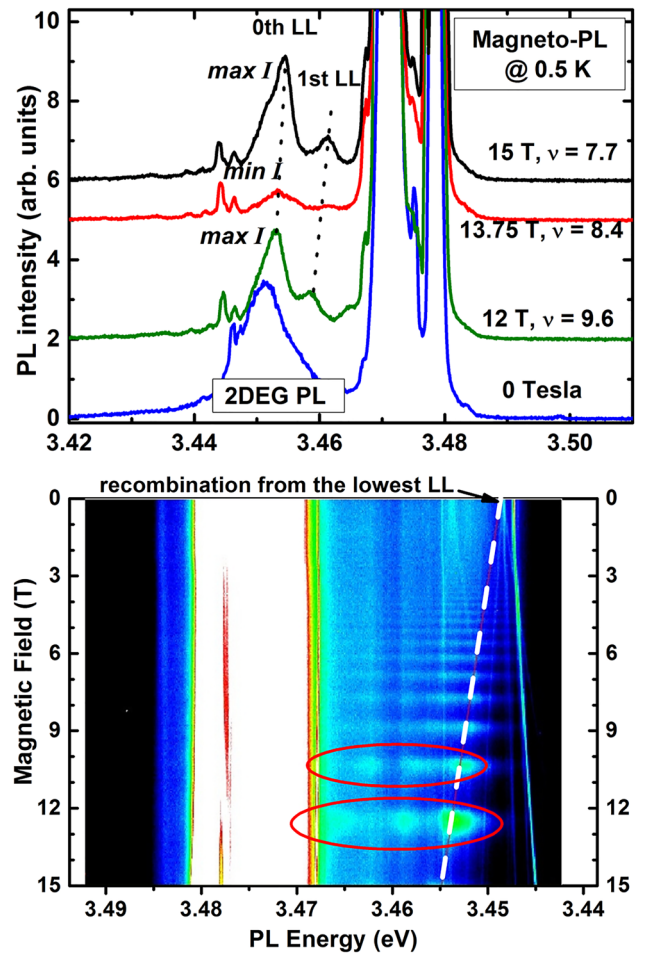


Fig. 3. Upper panel: Low-temperature magneto-PL data ($T=0.5\text{K}$) of the GaN/AlGaN heterostructure. At magnetic fields $>10\text{T}$, clearly separated peaks with spacing proportional to the magnetic field in the energy region between 3.45 and 3.46 eV become visible, which are attributed to split Landau levels of the 2DEG. The dotted lines are a guide to the eye and follow the energetic positions of the two lowest LLs. Lower panel: Magneto-PL intensity plotted vs magnetic field and wavelength. Dark spots represent low intensity and bright ones high intensity regions. The dashed line following the lowest LL is a guide to the eye. At high fixed fields, multiple bright spots (encircled) are visible representing intensity changes due to LL splitting. The magnetic field-dependent intensity variations are discussed in Sec. III C and Fig. 5.

quantum transport. Clear zero resistance values at large fields exclude any parasitic conduction path. Zeeman splitting (lifting of the spin degeneracy within a spin-degenerate LL) commences and becomes clearly visible above 7 T. These features are not as pronounced for the optically detected intensity variations. Here, the oscillations commence at $\sim 3\text{T}$ with no signs of Zeeman splitting up to fields of 15 T. Neither the minima nor the maxima in magneto-PL intensity match the well-understood minima in the transport traces. While the exact mechanism of the variation in PL intensity is still not fully understood (but seems to originate from the electrostatic potential changes near the heterojunction and subsequent redistribution of the electron wave functions),²² it is interesting to note that its periodicity in $1/B$ is identical to its magnetotransport counterpart (Fig. 5, lower panel). From this frequency, a carrier density of $2.8 \cdot 10^{12}\text{cm}^{-2}$ can

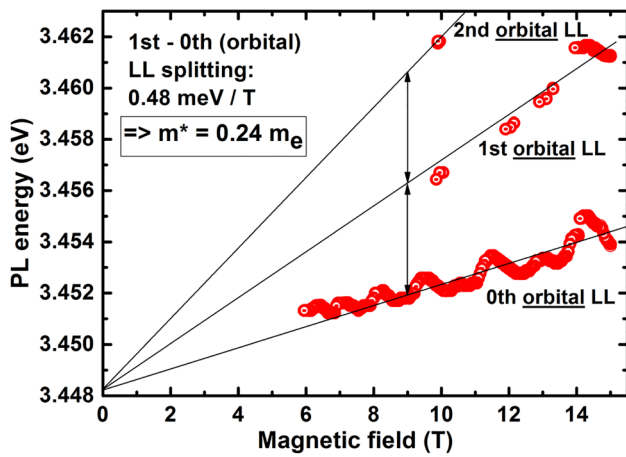


FIG. 4. Reconstructed Landau level fan from the energetic positions of the PL intensity maxima in Fig. 3 (lower panel). From the separation of the branches, an effective mass of the 2D electrons of $0.24m_0$ can be extracted.

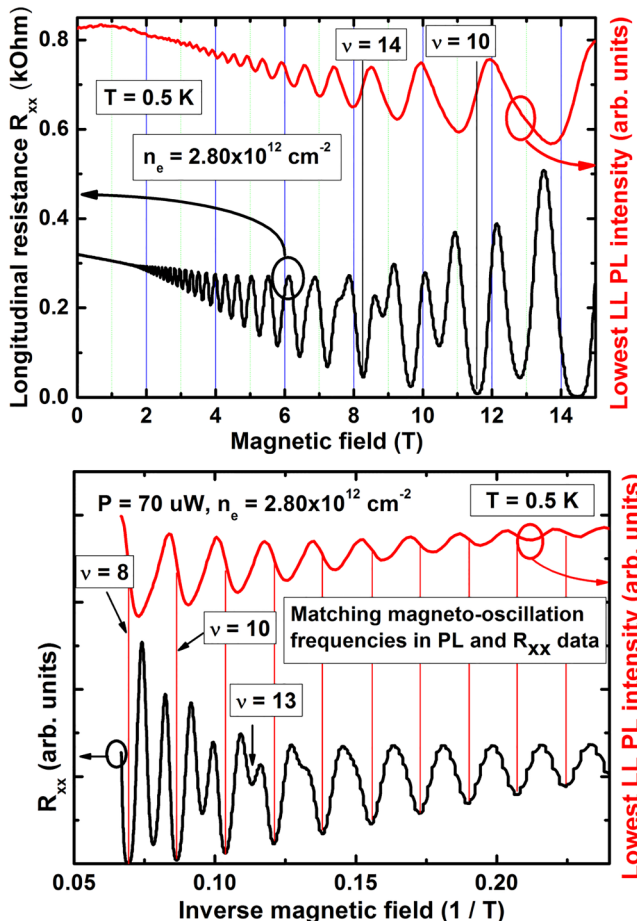


FIG. 5. Upper panel: Simultaneously recorded Shubnikov-de Haas (lower trace) and PL oscillations (upper trace) at 0.5 K under steady UV illumination. The well-understood minima in the electrical case do not match with their PL counterparts. Lower panel: Despite the mismatch of the minima, the oscillation frequency in the $1/B$ plot is identical for both cases, resulting in a 2DEG carrier density of $2.8 \cdot 10^{12} \text{ cm}^{-2}$. The LL filling factors are extracted from the magnetotransport data for both panels.

be derived. Since magneto-PL is only sensitive to the 2DEG density and not to all conduction paths, it represents a noninvasive and contactless method of determining the 2D carrier density whenever other electrical methods fail, e.g., due to processing or contact issues, or heavy parasitic conduction. While simultaneous recording of both oscillation types was previously barely possible for GaAs- or ZnO-based material, those measurements seemingly work flawlessly for the case of the GaN/AlGaN system. One possible reason could be the channel density robustness under heavy optical excitation, which has been recently described in detail.²⁰

IV. SUMMARY AND CONCLUSIONS

Landau level splitting in the density of states was observed in magneto-PL spectra for two-dimensional electrons confined in an ultrapure GaN/AlGaN heterostructure grown on bulk GaN. From the reconstructed LL fan, an effective electron mass of $0.24m_0$ could be extracted. The combination of ultrapure GaN grown on bulk GaN yields record narrow excitonic line widths of $100 \mu\text{eV}$ and atomically flat surfaces, both originating from a low substrate defect density. A direct comparison of simultaneously recorded magnetoresistance and magneto-PL oscillations yields identical 2DEG density for both oscillation types. The magneto-optical determination of the 2D carrier density represents a noninvasive and contactless measurement when other electrical methods fail.

ACKNOWLEDGMENTS

The TU Dresden part of the work was partially funded by the Deutsche Forschungsgemeinschaft (DFG, German Research Foundation)—Project No. 348524434. V.V.S. and I.V.K. acknowledge the support from the Russian Science Foundation (Grant No. 19-42-04119). The NaMLab gGmbH part was financially supported by the German Federal Ministry of Education and Research-BMBF (Project “ZweiGaN,” No. 16ES0145K) and the German Federal Ministry of Economics and Technology-BMWi (Project No. 03ET1398B).

¹K. J. Chen, O. Häberlen, A. Lidow, C. I. Tsai, T. Ueda, Y. Uemoto, and Y. Wu, *IEEE Trans. Electron Devices* **64**, 779 (2017).

²H. Amano *et al.*, *J. Phys. D Appl. Phys.* **51**, 163001 (2018).

³A. V. Shchepetilnikov, D. D. Frolov, V. V. Solov'yev, Yu. A. Nefyodov, A. Großer, T. Mikolajick, S. Schmult, and I. V. Kukushkin, *Appl. Phys. Lett.* **113**, 052102 (2018).

⁴M. J. Manfra, K. W. Baldwin, A. M. Sergent, K. W. West, R. J. Molnar, and J. Caissie, *Appl. Phys. Lett.* **85**, 5394 (2004).

⁵H. T. Chou, S. Lüscher, D. Goldhaber-Gordon, M. J. Manfra, A. M. Sergent, K. W. West, and R. J. Molnar, *Appl. Phys. Lett.* **86**, 073108 (2005).

⁶H. T. Chou, D. Goldhaber-Gordon, S. Schmult, M. J. Manfra, A. M. Sergent, and R. J. Molnar, *Appl. Phys. Lett.* **89**, 033104 (2006).

⁷K. von Klitzing, G. Dorda, and M. Pepper, *Phys. Rev. Lett.* **45**, 494 (1980).

⁸I. V. Kukushkin and S. Schmult, *JETP Lett.* **101**, 693 (2015).

⁹V. V. Solov'yev and I. V. Kukushkin, *Phys. Rev. B* **96**, 115131 (2017).

¹⁰J. P. Bergman, T. Lundström, B. Monemar, H. Amano, and I. Akasaki, *Appl. Phys. Lett.* **69**, 3456 (1996).

¹¹J. P. Zhang, D. Z. Sun, X. L. Wang, M. Y. Kong, Y. P. Zeng, J. M. Li, and L.-Y. Lin, *Appl. Phys. Lett.* **73**, 2471 (1998).

- ¹²N. Akopian *et al.*, *Appl. Phys. Lett.* **94**, 223502 (2009).
- ¹³D. Jana and T. K. Sharma, *J. Phys. D Appl. Phys.* **49**, 265107 (2016).
- ¹⁴B. Monemar, J. P. Bergman, and P. O. Holtz, *Appl. Phys. Lett.* **76**, 655 (2000).
- ¹⁵F. Schubert, S. Wirth, F. Zimmermann, J. Heitmann, T. Mikolajick, and S. Schmult, *Sci. Technol. Adv. Mater.* **17**, 239 (2016).
- ¹⁶S. Schmult, F. Schubert, S. Wirth, A. Großer, T. Mittmann, and T. Mikolajick, *J. Vac. Sci. Technol. B* **35**, 02B104 (2017).
- ¹⁷R. Hentschel, J. Gärtner, A. Wachowiak, A. Großer, T. Mikolajick, and S. Schmult, *J. Cryst. Growth* **500**, 1 (2018).
- ¹⁸K. Kornitzer *et al.*, *Phys. Rev. B* **60**, 1471 (1999).
- ¹⁹D. Pohl, V. V. Solovyev, S. Röher, J. Gärtner, I. V. Kukushkin, T. Mikolajick, A. Großer, and S. Schmult, *J. Cryst. Growth* **514**, 29 (2019).
- ²⁰S. Schmult, S. Wirth, V. V. Solovyev, R. Hentschel, A. Wachowiak, A. Großer, I. V. Kukushkin, and T. Mikolajick, eprint [arXiv:1812.07942](https://arxiv.org/abs/1812.07942) (2018).
- ²¹M. J. Manfra, K. W. Baldwin, A. M. Sergent, R. J. Molnar, and J. Caissie, *Appl. Phys. Lett.* **85**, 1722 (2004).
- ²²A. Babinski, M. Potemski, and H. Shtrikman, *Phys. Rev. B* **65**, 233307 (2002).